



A novel UAV-based approach for biomass prediction and grassland structure assessment in coastal meadows

M. Villoslada Peciña^{a,*}, T.F. Bergamo^a, R.D. Ward^{a,b}, C.B. Joyce^b, K. Sepp^a

^a Institute of Agriculture and Environmental Sciences, Estonian University of Life Sciences, Kreutzwaldi 5, EE-51006 Tartu, Estonia

^b Centre for Aquatic Environments, University of Brighton, Cockcroft Building, Moulsecoomb, Brighton BN2 4GJ, United Kingdom

ARTICLE INFO

Keywords:

UAV
Coastal plant communities
Above-ground biomass
Sward structure
Ecosystem services

ABSTRACT

Coastal meadows provide a wide range of ecosystem services worldwide. In order to better target conservation efforts in these ecosystems, it is necessary to develop highly accurate models that account for the spatial nature of ecosystem structure, processes and functions. In this study, above-ground biomass was predicted at very high spatial resolution in nine study sites in Estonia. A combination of UAV-derived datasets were used to produce vegetation indices and micro topographic models. A random forest algorithm was used to generate above-ground biomass maps and assess the contribution of each predictor variable. The model successfully predicted above-ground biomass at very high accuracies. Additionally, grassland structural heterogeneity was assessed using UAV-derived datasets and vegetation indices. The results were subsequently related to management history at each study site, showing that continuous, monospecific grazing management tends to simplify grassland structure, which could in turn reduce the supply of a key regulation and maintenance ecosystem services: nursery and reproduction habitat for waders. These results also indicate that UAV-based surveys can serve as reliable grassland monitoring tools and could aid in the development of site-specific management strategies.

1. Introduction

Coastal meadows are wetlands with an abundance of grasses subject to high water levels or flooding (Joyce et al., 2016). These valuable ecosystems have been recognized for the provision of a wide range of ecosystem services (ES) worldwide (Barbier et al., 2011; Salomidi et al., 2012). Primary production in coastal meadows is a key ecosystem function that drives the supply of ES such as carbon (C) sequestration as well as food provision for livestock. Vegetated coastal environments are well-noted for their capacity to retain carbon both from allochthonous sources and through absorbing atmospheric CO₂ through primary productivity, which exceeds respiration rates (Duarte et al., 2013; Ward, 2020a). The authors of the previous study estimated that an average of 4.8–87.3 Tg/yr of C are sequestered globally in saltmarshes, and 0.4–6.5 Pg of C are stored in saltmarsh soils. Moreover, coastal meadows are characterized by long-term C burial due to low decomposition rates as a result of anoxic conditions in their soils (Enríquez et al., 1993; Mcleod et al., 2011).

Beyond their role as carbon sinks, coastal meadows maintain nursery populations and habitats for waders (Rhymer et al., 2010), which constitutes another essential regulation and maintenance ecosystem service

(Haines-Young and Potschin, 2018) supplied by these ecosystems. The high species diversity and complex structure of coastal meadow landscapes comprise an important habitat for populations of wildfowl, waders, amphibians (Rannap et al., 2017), and arthropods (Torma et al., 2019). The structural heterogeneity of swards in coastal meadows is mostly determined by low intensity grazing (Verhulst et al., 2011), which simultaneously maintains high levels of plant species richness (Burnside et al., 2007; Ward et al., 2016b). Extensive grazing maintains heterogeneous patches of vegetation, providing nesting and feeding areas for a variety of species (Leito et al., 2014; Aldabe et al., 2019) such as Common Redshank (*Tringa totanus*) (Sharps et al., 2016), Lapwing (*Vanellus vanellus*) and Eurasian curlew (*Numenius arquata*) (Tichit et al., 2005; Żmihorski et al., 2018). In addition to the increased habitat availability, long term grazing in coastal wetlands also limits rates of denitrification and increases microbial immobilization of C in soils, therefore enhancing nutrient availability and the capacity of soils to store C (Olsen et al., 2011).

Coastal meadows supply a wide array of other essential ecosystem services. Among these, wave attenuation, sediment bio-stabilization, water regulation and filtration and storage of nutrients and contaminants (Barbier, 2013) have been identified as fundamental elements of

* Corresponding author at: Kreutzwaldi 5, room 2c18, Tartu 51006, Estonia.
E-mail address: mpecina@emu.ee (M. Villoslada Peciña).

<https://doi.org/10.1016/j.ecolind.2020.107227>

Received 23 April 2020; Received in revised form 29 October 2020; Accepted 27 November 2020

Available online 22 December 2020

1470-160X/© 2020 The Author(s).

Published by Elsevier Ltd.

This is an open access article under the CC BY-NC-ND license

(<http://creativecommons.org/licenses/by-nc-nd/4.0/>).

coastal landscapes. Recreation, cultural heritage, aesthetic values and educational values have also been listed as cultural ecosystem services highly valued by societies (Martin et al., 2016). Despite their multifunctional character, coastal wetlands, including meadows, have been identified as a particularly sensitive ecosystem to Global Change, mainly due to increased sea level (Ward et al., 2016b; Ward, 2020b), increased sea and ocean temperatures and altered atmospheric circulation patterns (Ward et al., 2016c) resulting in increased frequency of storms (Thorne et al., 2012; Spalding et al., 2014; Ward et al., 2014; Lima et al., 2020). In addition to the threats posed by altered climate patterns, coastal meadows have undergone degradation in the form of agricultural intensification in many areas and abandonment in others (Henle et al., 2008). In the absence of management, coastal meadows become dominated by tall-sward communities (Clausen et al., 2013), which in turn leads to decreased availability of adequate habitat for waterbirds (Vulink et al., 2010). Moreover, abandoned coastal meadows are characterized by a higher presence of less digestible plants (Summers et al., 1993), which hinders the reintroduction of grazing activities. In this regard, Clausen et al. (2013) point out that adequate grassland management may counteract the effects of climate change by balancing the expected areal loss of coastal meadows due to sea level rise.

The complex dynamics of coastal wetlands and their sensitivity to Global Change call for robust monitoring techniques, able to account for the spatial dimension of ecosystems structures, processes and functions. For instance, it is essential to understand how the patterns of biomass production change spatially in coastal wetlands, as this may provide a better understanding of responses to global change (Doughty and Cavanaugh, 2019). In addition, spatially explicit monitoring schemes could provide valuable insights on the combined effects of Climate Change and grassland abandonment and their impacts on the availability and quality of habitat for wader populations. Some initiatives such as GEOBON have highlighted the need to integrate Earth Observation (EO) with in-situ observations in order to adequately model the status and trends of essential biodiversity variables like net primary productivity, disturbance regimes, habitat structure or ecosystem extent and fragmentation (Vihervaara et al., 2017). In this regard, the rapid development of EO platforms and sensors has led to an unprecedented availability of high quality remotely sensed data. For instance, several studies have used passive remote sensing data derived from satellite sensors to map salt-marsh plant communities (Akumu et al., 2010; Kumar and Sinha, 2014), mangroves extent (Giri et al., 2010) and biomass production in coastal wetlands (O'Donnell and Schalles, 2016; Mafi-Gholami et al., 2018). However, satellite-derived EO data may not provide the spatial resolution required to account for the fine scale patterns and heterogeneous structure of grassland swards (Ward et al., 2013; Villoslada et al., 2020). This could in turn hamper the operationalization of remote sensing techniques for grassland management and conservation purposes. On the other hand, the emergence of UAVs and lightweight sensors in the last decade has revolutionized ecological and environmental monitoring (Baena et al., 2018; Baxter and Hamilton, 2018). While providing very high spatial detail, UAVs are also able to survey large areas repeatedly. This has resulted in a wide variety of applications including nature conservation, forestry, ecology and precision agriculture (Adão et al., 2017). Several authors have demonstrated the successful use of UAVs as a tool for nature management and conservation. For instance, UAV-based vegetation monitoring has been used to target restoration efforts in Algarrobo forests in Peru (Baena et al., 2018). Similarly, UAVs have been used to detect and quantify invasive knotweed species (Martin et al., 2018). Efforts to monitor habitat degradation in protected areas have also benefitted from the use of UAVs (López and Mulero-Pázmány, 2019). Specifically in the field of grassland and coastal wetland ecology, UAVs combined with multispectral sensors have been used to map plant communities (Villoslada et al., 2020), quantify biomass production (Doughty and Cavanaugh, 2019), monitor tidal morphodynamics (Taddia et al., 2019) and monitor long-term ecological integrity (Díaz-Delgado et al., 2018).

These approaches commonly utilize the spectral properties of vegetation in order to predict plant communities' spatial distribution patterns and structure (Veettil et al., 2020). In addition to multispectral data, aerial photogrammetry has been used to map hydrological features and plant community structure in saltmarshes (Kalacska et al., 2017; Meng et al., 2017). These increasingly diverse sources of remotely sensed data call for processing and analysis frameworks able to handle highly dimensional datasets and unveil complex ecosystem patterns. In this regard, machine and deep learning techniques offer an efficient solution to process large spatial datasets (Lary et al., 2016). For instance, random forest (RF) is a supervised algorithm that has been increasingly used to map and predict both discrete clusters such as plant communities (Villoslada et al., 2020) as well as continuous variables such as biomass (Mutanga et al., 2012) and tree attributes (Yu et al., 2011).

Despite all the recent advances in earth observation tools and techniques, there still is a lack of highly detailed, spatially explicit data on the structural patterns and primary productivity of coastal meadow in relation to management (Villoslada et al., 2020). While current monitoring schemes in grasslands rely on *in situ* data collection and frequent field surveys (Ali et al., 2016), the fusion of the former with UAV-based assessments could provide valuable new knowledge for grassland restoration, management and conservation. Some authors (Baena et al., 2017) have highlighted the need to combine traditional plot-based vegetation survey methods with UAV surveys to acquire deeper knowledge on ecosystem structure and dynamics.

In order to develop adequate monitoring strategies and improve targeted management actions, this study develops a methodology to operationalize UAVs as tools to monitor vegetation and ecosystem functioning in coastal meadows. By utilizing multiple UAV-derived remote sensing products, the study addresses fine-scale patterns and dynamics of ecosystem functioning in coastal meadows. More specifically, the aims of the present study are:

1. To generate very high spatial resolution maps of standing above-ground biomass in Boreal Baltic coastal meadows in Estonia based on UAV multispectral imagery and aerial photogrammetry.
2. To assess the grassland sward structure in Boreal Baltic coastal meadows in Estonia based on UAV multispectral imagery and aerial photogrammetry.
3. To assess the effect of the duration and type of management regime on coastal meadows sward structure.

2. Methods

2.1. Study sites

Coastal landscapes in the Baltic Sea region are variable and exhibit considerable geographical differences. The northern Baltic Sea consists of erosion-resistant crystalline rock outcrops, while the southern section consists of sedimentary rocks superimposed on crystalline rocks (Rivis et al., 2016). Estonia is located between these two distinct zones. The narrow connection with the Atlantic Ocean through the Danish Straits and the resultant isolation of the Baltic Sea means sea water salinity is classified as brackish (Kont et al., 2003). Coastal wetlands in Estonia are characterized by a very low tidal range (~0.02 m range), and flooding is predominantly driven by atmospheric pressure and fluctuating meteorological conditions across the North Atlantic and Fennoscandia (Suursaar and Sooäär, 2007). As a result, the rate and magnitude of inundation is irregular and varies throughout the coastal landscape (Rivis et al., 2016). Coastal wetlands in Estonia include many plant communities with rare and protected species and considerable biodiversity, supporting breeding and migratory fauna (Berg et al., 2012; Rivis et al., 2016). These wetlands are maintained by regular management, usually in the form of low intensity grazing or mowing (Berg et al., 2012).

The study was undertaken in nine study sites located across the

Western coast of Estonia: In the Silma Nature Reserve (3 sites: Tahu North (TN), Tahu South (TS) and Kudani (Kd)), Matsalu National Park (2 sites: Matsalu1 (M1) and Matsalu2 (M2)) and Vormsi Island (4 sites: Rumpo East (RE), Rumpo West (RW), Hosby (Hb), and Rälby (Rb)). Fig. 1 represents the location of all study sites within Silma Nature Reserve and Vormsi Island (A) and Matsalu National Park (B). The choice of sites responds to the need of assessing the widest possible range of management options, considering livestock species, grazing load and management duration. Moreover, all sites constitute strategic locations along the East Atlantic bird migratory route (Palm et al., 2017) and are located within protected areas of national and regional relevance.

2.2. Data processing and analysis

Fig. 2 outlines the methodological steps undertaken to achieve the three objectives of the study. The workflow is divided into three general steps including data collection, pre-processing and processing. Data collection includes the acquisition of both UAV-based remotely sensed data and above-ground biomass samples in the field. Pre-processing comprises all the steps needed to transform raw remotely sensed products into georeferenced and interpretable datasets. Ultimately, the processing section encompasses all the algorithms required to model above-ground biomass, describe grassland sward structure and assess the effects of grassland management in sward complexity.

2.3. Field data collection

2.3.1. Plant communities and biomass sampling

Field sampling was undertaken in July 2019 during a period of two weeks. The sampling methodology follows the phytosociological classification developed by Burnside et al. (2007). The authors identified seven main plant communities considering the indicator species for

Estonian coastal wetlands: Reed swamp, Clubrush swamp, Lower shore meadow, Upper shore meadow, Open pioneer, Tall grass and Scrub and developing Woodland. Because of their peripheral occurrence in coastal meadows, the present study excludes Reed Swamp, Clubrush Swamp and Scrub and developing Woodland from the analysis. Table 1 describes the communities under study, their occurrence and key species.

Following a stratified random approach, twenty above-ground biomass samples per community type per site were collected. The above-ground biomass samples were subsequently divided into two datasets: a training dataset (10 samples per site per community type) and a validation dataset (ten samples per site per community type). These two datasets constitute an essential component of the supervised modelling and mapping process (Fig. 2). Due to different site characteristics and management regimes, not all communities are present in all sites. The aboveground sampling of plant communities at the study sites (TN: 3 communities, TS: 3 communities, Kd: 4 communities, M1: 4 communities, M2: 4 communities, Rb: 4 communities, Hb: 2 communities, RW: 2 communities, RE: 3 communities). This resulted in a total of 520 aboveground biomass samples collected using a 30 × 30 cm quadrat.

X, Y and Z coordinates were recorded within all quadrats using a Sokkia GSR2700 ISX dGPS. Points were recorded in the corners and centre of all quadrats, five points per quadrat (Ward et al., 2013). Biomass was cut at ground level and samples were subsequently dried at 70 °C for 48 h and weighed.

2.3.2. Image acquisition

Multispectral images covering the extent of each study site were collected using a Sensefly Ebee UAV equipped with a Parrot Sequoia 1.2 megapixel monochromatic multi-spectral sensor. Images were collected in four spectral bands: Green (530–570 nm), red (640–680 nm), red edge (730–740 nm) and near infrared (770–810 nm). Images were captured

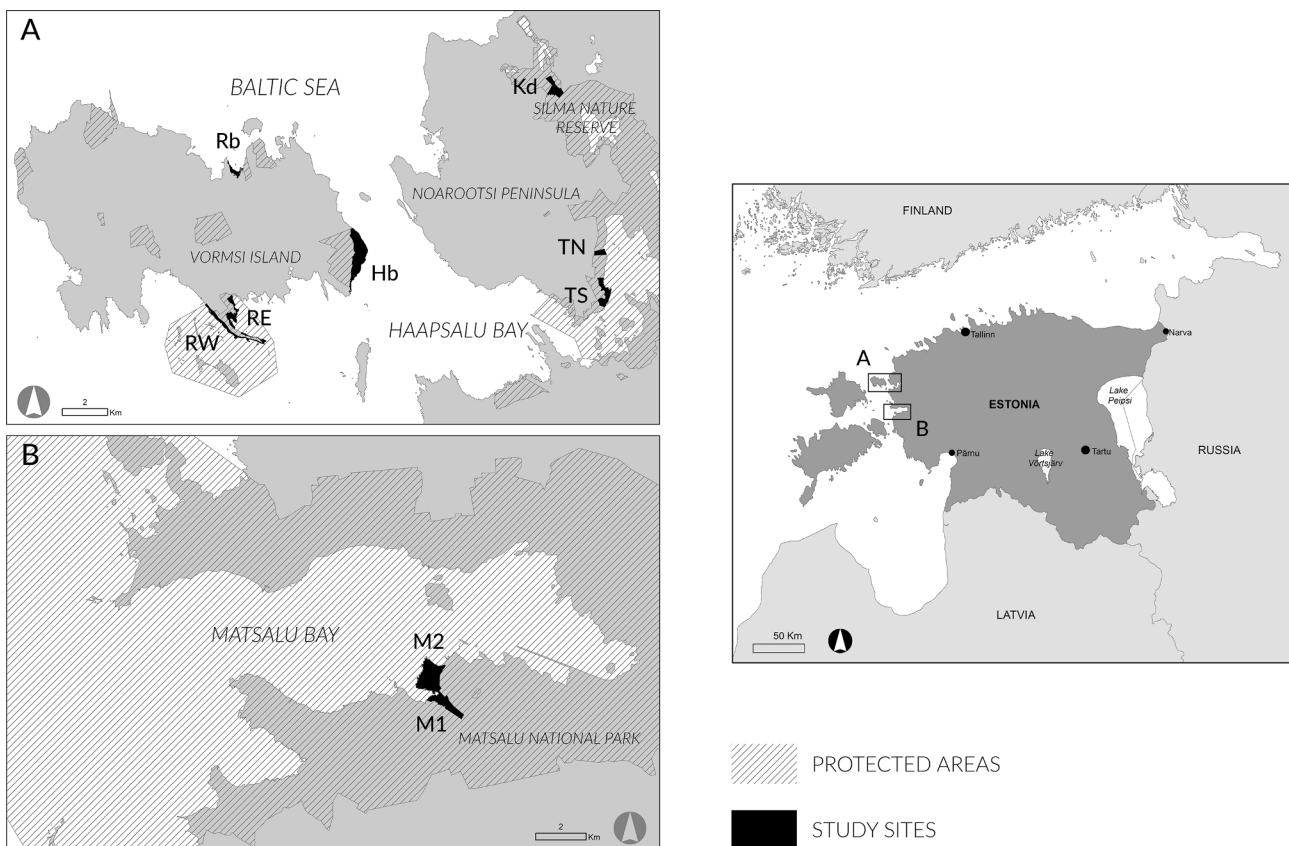


Fig. 1. Location of the study sites within the Silma Nature Reserve (A), Vormsi Island (A) and Matsalu National Park (B) in West Estonia. M1: Matsalu 1; M2: Matsalu 2; TN: Tahu North; TS: Tahu South; Kd: Kudani; RE: Rumpo East; RW: Rumpo West; Rb: Rälby; Hb: Hosby.

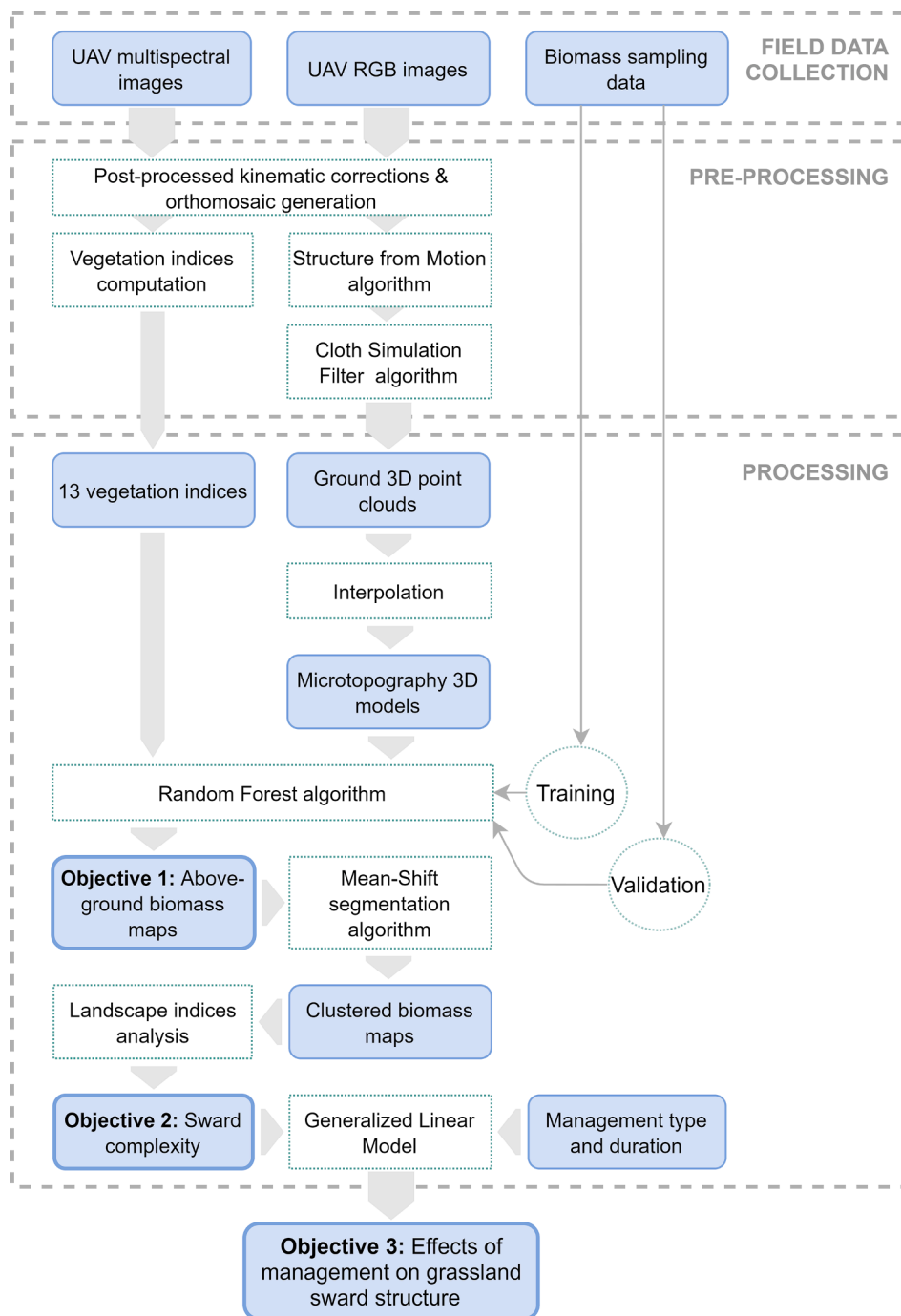


Fig. 2. Flowchart illustrating the methodological steps undertaken in this study.

at a flight height of 120 m, with a 10 cm pixel resolution and prior to each flight an Airinov calibration panel was used to radiometrically correct images.

Each multispectral flight was followed by a photogrammetric flight. RGB images were captured using a senseFly S.O.D.A camera at a flight height of 123 m with a resolution of 3.5 cm per pixel. The datasets derived from both multispectral and RGB images were subsequently used as prediction covariates within the modelling process (Fig. 2).

2.4. Image processing and analysis

All collected images underwent a post-processed kinematic (PPK) correction process in eMotion 3®. RINEX observation and navigation files from the ESTPOS Estonian GNSS-RTK permanent stations network

were used to increase positional accuracy of the multispectral and rgb images (Tadrowski, 2014). The positional accuracy achieved after this process is under 7 cm, as tested by Villoslada et al. (2020). After positional corrections, multispectral and rgb orthomosaics were constructed in Pix4D v.4.3.31®. A total of five orthomosaics were obtained for each study site.

2.5. Vegetation indices

The multispectral orthomosaics were used to compute 13 vegetation indices (Table 2). Vegetation indices convey spectral information related to photosynthetic activity, vegetation vigour, status and coverage (Filho et al., 2020) and therefore constitute valuable predictors for modelling essential ecosystem functions. In the present study, the

Table 1

Plant communities under study and their indicator species. M1: Matsalu 1; M2: Matsalu 2; TN: Tahu North; TS: Tahu South; Kd: Kudani; RE: Rumpo East; RW: Rupo West; Rb: Rälby; Hb: Hosby.

Community	Key Species	Sites	Description
Open Pioneer	<i>Salicornia europaea</i> , <i>Suaeda maritima</i>	M1, M2, Kd	The open pioneer community is found in localised depressions and is characterized by a high frequency and abundance of bare ground and high salt concentration due the evaporite accumulation.
Lower Shore	<i>Juncus gerardii</i> , <i>Plantago maritima</i>	M1, M2, TN, TS, Kd, RE, RW, Rb, Hb	The lower shore community tends to establish on low-lying land where periodic flooding is influential (Ward et al., 2013) and it is indicated by dominant <i>Juncus gerardii</i> with frequent <i>Festuca rubra</i> , <i>Glaux maritima</i> , <i>Plantago maritima</i> , <i>Triglochin maritimum</i> , bare ground and litter.
Upper Shore	<i>Festuca rubra</i> , <i>Leontodon autumnalis</i>	M1, M2, TN, TS, Kd, RE, RW, Rb	The upper shore community is denser than Lower Shore vegetation and relatively more species-rich. <i>Festuca rubra</i> is dominant with frequent <i>Leontodon autumnalis</i> and <i>Triglochin maritimum</i> .
Tall Grass	<i>Elytrigia repens</i> , <i>Festuca arundinacea</i>	M1, M2, TS, Kd, RE, RW, Rb, Hb	Tall grass vegetation is located at a higher elevation than upper shore where flooding is less pronounced (Ward et al., 2013) and it is one of the most species-rich Estonian wetland plant communities with an abundance of <i>Elytrigia repens</i> , <i>Festuca</i> spp. and plant litter (Burnside et al., 2007).

selection of indices was based on their ability to detect changes in vegetation status, pigment content and plant productivity. Among the selected indices, Green Red Difference Index (GRDI) and Green Difference Index (GDI) have been previously used due to their ability to predict the percentage of green herbage (Gianelle and Vescovo, 2007, Villoslada et al., 2020). Indices incorporating the red-edge band (NDVire, SRre, RTVcore and Datt4 in this study) have been used to produce highly accurate predictions of biomass due to their ability to overcome saturation (Mutanga and Skidmore, 2004). Similarly, Difference Vegetation Index (DVI) has been used to discern the large amount of variance in biomass predictions (Maguigan et al., 2016). Soil Adjusted Vegetation Index (SAVI) and Modified Soil Adjusted Vegetation Index (MSAVI) were chosen due to their ability to compensate for the effect of soil in sparsely vegetated areas (Ren et al., 2011). Band ratios like Green Ratio Vegetation Index (GRVI) are known to correlate well with wetland vegetation biomass (Naidoo et al., 2019). Normalized Difference Vegetation Index (NDVI), Green Normalized Vegetation Index (GNDVI) and 2-band Enhanced Vegetation Index (EVI2) have shown high correlations with grassland biomass in previous studies (Jing et al., 2014; Naidoo et al., 2019).

2.6. Microtopography 3D models

In coastal meadows, microtopography plays a key role in the distribution of soil moisture gradients and availability of nutrients (Ward et al., 2016a). In order to test and improve above-ground biomass prediction accuracies, microtopography was included in the ensemble of explanatory variables. In order to obtain microtopography models at each study site, a Structure-from Motion (SfM) algorithm was implemented. SfM generates 3D point clouds from a set of photographs. As described by Westoby et al. (2012), the SfM process encompasses three

Table 2

List of vegetation indices selected in the present study to predict standing above-ground biomass.

Vegetation index	Equation	Reference
Normalized Difference Vegetation Index (NDVI)	$(NIR-R)/(NIR+R)$	Rouse et al. (1974)
Soil Adjusted Vegetation Index (SAVI)	$[(NIR-R)/(NIR+R+L)](1+L)$	Huete (1988); Ullah et al. (2012)
Modified Soil Adjusted Vegetation Index (MSAVI)	$L(\text{soil adjustment factor}) = 0.5[2NIR + 2 - \sqrt{(2NIR+1)^2 - 8(NIR-R)}]$	Qui et al. (1994); Jing et al. (2014)
2-band Enhanced Vegetation Index (EVI2)	$2.5[(NIR-R)/(NIR+2.4R+1)]$	Jiang et al. (2008); Jing et al. (2014)
Difference Vegetation Index (DVI)	$NIR-\alpha R$ $\alpha = 0.96916$	Richardson & Everitt (1992); Maguigan et al. (2016)
Green Normalized Vegetation Index (GNDVI)	$(NIR-G)/(NIR+G)$	Gitelson et al. (1996); Naidoo et al. (2019)
Green Ratio Vegetation Index (GRVI)	NIR/G	Sripada et al. (2006); Naidoo et al. (2019)
Green Difference Index (GDI)	$NIR-R+G$	Gianelle and Vescovo (2007)
Green Red Difference Index (GRDI)	$(G-R)/(G+R)$	Gianelle and Vescovo (2007)
Red edge normalized difference vegetation index (NDVire)	$(NIR-Rededge)/(NIR+Rededge)$	Gitelson and Merzlyak (1994); Kross et al. (2015)
Red edge simple ratio (SRre)	$NIR/Rededge$	Gitelson and Merzlyak (1994); Kross et al. (2015); Naidoo et al. (2019)
Red edge triangular vegetation index (core only) (RTVcore)	$100(NIR-Rededge)-10(NIR-G)$	Kross et al. (2015); Clausen et al. (2013)
Datt4	$R/G \cdot Rededge$	Datt (1998)

essential steps. The first steps requires the detection of common key points across a set of images using the Scale Invariant Feature Transform (SIFT). Secondly, a low-density 3D point cloud is extracted based on camera locations and orientations. The point cloud is subsequently densified based on triangulation and incremental reconstruction. The third step involves the transformation from a relative to an absolute 3D coordinate system, post-processing of the dense point clouds and transformation into a raster DEM.

The three-step process described by Westoby et al. (2012) was implemented in this study utilizing Pix4Dmapper in combination with CloudCompare. Pix4Dmapper was used to detect matching points between all RGB images at each study site and subsequently generate a dense 3D point cloud. Pix4Dmapper combines the SfM algorithm with the Multi-View stereo photogrammetry (SfM-MVS) (Smith et al., 2015) to detect common features in the images and construct a 3D scene based on bundle adjustment (Smith et al., 2015). The dense point clouds were then imported into CloudCompare in order to classify points into ground and non-ground classes. Within CloudCompare, the Cloth Simulation Filtering (CSF) algorithm allows for an efficient computation of the ground surface and separation of vegetation from soil (Zhang et al., 2016). The CSF algorithm uses a cloth simulation technique (Zhang et al., 2016) and the inversion of the original point cloud. By modifying two parameters, namely an integer parameter "rigidness" and a Boolean parameter "ST", the user defines the way the simulated cloth lies over the inverted point cloud and ultimately determines the way points are classified. Compared to other point classification techniques, the CSF algorithm offers reliable classification results with few parameters

(Zhang et al., 2016).

A raster digital terrain model (DTM) was computed at each study site by selecting and interpolating the points classified as ground by the CSF algorithm. Point interpolations and rasterization were undertaken in CloudCompare.

2.7. Supervised above-ground biomass prediction

In order to predict aboveground biomass in coastal meadows at the study sites, a RF machine learning classifier for the prediction of continuous variables was implemented in R (v3.5.1).

The R packages used to perform RF were:

- ModelMap package: used to generate prediction maps based on training datasets and validate the models with independent test sets and Out Of Bag (OOB) predictions (Freeman et al., 2009).
- raster package: used to enable reading, manipulating, analysing and modelling gridded spatial datasets (Hijmans and van Etten, 2012).
- randomForest package: used to build random forest models for regression based on a forest of decision trees using random inputs (Liaw and Wiener, 2002).
- ROCR package: used to transform the input data into a standardized format (Sing et al., 2005).

For each study site, two separate random forest models were run: a model including only vegetation indices as explanatory variables and a model combining vegetation indices with microtopography DTMs. All pixels falling within each of the 260 sampling quadrats were assigned to the corresponding above-ground value recorded at each quadrat and utilized as the training dataset. Additionally, 260 duplicates were used as a validation dataset.

2.8. Validation and accuracy assessment

Explained variance (R^2) and root mean square error (RMSE) were used to test the accuracy of RF biomass predictions over the nine study sites. All accuracy tests were run using the validation dataset and a 95% confidence interval of RMSE. In addition, the prediction performance of each explanatory variable was assessed using percent increase in Mean Squared Error (MSE) (Breiman, 2001; Mutanga et al., 2012).

The percent increase in MSE is calculated as the increase in the OOB when one variable is permuted (Mutanga et al., 2012). This estimate of accuracy represents the degradation of the model predictive performance when one variable is permuted. The percent increase in MSE enables a ranking of the predictor variables to be conducted according to their contribution to the model performance.

2.9. Sward structure assessment

Grassland sward structure was evaluated using a combination of data clustering and landscape indices. In this study, sward structure is defined following the description by Laca and Lemaire (2000), as the distribution and arrangement of above ground plant material. In order to facilitate the characterization of grass swards, each above-ground biomass map was clustered into discrete grass units using a Mean-Shift segmentation algorithm (Comaniciu and Meer, 2002). The Mean-Shift segmentation algorithm groups together adjacent pixels with similar values by iteratively assigning each pixel with a peak of the image probability density (Zhou et al., 2011). Mean-Shift clustering routine is an unsupervised segmentation technique and does not require a priori knowledge of the number of output clusters (Comaniciu and Meer, 2002). The Mean-Shift clustering routine was implemented in QGIS v 3.12.

The clustered above-ground biomass maps were further analysed using a set of five landscape indices that characterize different components of landscape configuration, patch size and heterogeneity (table 3).

The landscape indices were calculated using the landscape-metrics package in R (Hesselbarth et al., 2019). In order to allow for statistical comparisons of grassland structure between study sites, each above-ground biomass cluster map was subsampled using fifteen 50 m diameter circular plots randomly located within each monitoring site map. Subsequently, landscape indices were calculated for each circular plot. A similar sampling procedure has been utilized by Plexida et al. (2014) at the landscape scale.

The clustering and landscape complexity approach used in this study facilitates the interpretation of continuous biomass data and enables descriptive assessments at the grassland plot level.

2.10. Effects of management history on sward complexity

In order to unveil the effects of management type, duration and intensity on coastal meadow sward structure, information on the management history corresponding to each study site was collected (table 4). Although coastal meadows are sometimes mown as well as grazed, the selected sites in this study have only undergone grazing. During a series of interviews, land owners provided detailed information on the following parameters:

- Duration of continuous management after management was reinstated or grassland was restored
- Grazing load (Livestock Units (LU)/ha) during the last two years
- Livestock species present in the grassland during all management history (cattle, sheep, horses or mixed)
- Livestock species present during the last two years of management (cattle, sheep or horses)

Kudani was excluded from the analysis due to lack of information on management.

In order to assess the effects of management on sward structure, a Generalized Linear Model (GLM) with gaussian distribution was applied using the GLM base function in R. GLM was chosen due to its ability to fit linear models to datasets that represent counts (e.g. grazing loads) or percentages (e.g. largest patch index), as well as assess the simultaneous effect of continuous and categorical variables (Zuur et al., 2009). The model distribution was selected following the criteria of minimizing the Akaike's information criterion (AIC) (Nolte et al., 2014). The five landscape indices described in section 2.8 were included as response variables, and years of management, present grazing load and livestock species (both past and present) included as explanatory variables. Two-way interaction functions were also included in the model. Additionally, Mann Whitney U-tests were implemented in R in order to compare the values of landscape indices between meadows with different herbivore species.

3. Results

3.1. Above-ground biomass prediction maps

Above-ground biomass was modelled in nine high resolution maps

Table 3
Landscape indices used to describe grassland structure at each study site.

Landscape index	Description
Patch average area (area_mn)	Mean area of all patches in the landscape under assessment
Patch density (pd)	Number of patches per area unit. Describes landscape fragmentation and heterogeneity
Edge density (ed)	Length of all edges in the landscape per area unit. Describes landscape fragmentation and heterogeneity
Landscape shape index (lsi)	Ratio between total edge length and the hypothetical minimum edge length. LSI is a landscape aggregation metric
Largest patch index (lpi)	Percentage of the landscape covered by the largest patch within the landscape under assessment

Table 4
Parameters describing grazing management history at each study site.

Site	Duration of management (years)	LU/ha (during the last two years)	Livestock species (management history)	Herbivore species (last two years)
Tahu N	9	1	Cattle	Cattle
Tahu S	9	1	Cattle	Cattle
Matsalu 1	39	0.8	Cattle	Cattle
Matsalu 2	39	0.72	Cattle	Cattle
Rumpo W	19	0.55	Mixed	Cattle
Rumpo E	15	1	Mixed	Cattle
Hosby	15	0.38	Mixed	Horses
Rälby	15	1.13	Mixed	Cattle

corresponding to the nine study sites (Fig. 3). Both RMSE and R² revealed high prediction accuracies for the random forest algorithm for all nine biomass prediction maps. RMSE ranged from 64.36 gr/m² in Matsalu 2 to 6.2 gr/m² in Rumpo E (Table 5), whereas R² ranged from 0.63 in Kudani to 0.98 in Hosby. The incorporation of digital terrain models in the explanatory variables dataset improved the prediction accuracy at all sites except Tahu N. Due to a failure during the survey flight, the digital terrain model could not be computed for Rälby.

SfM-derived digital terrain models were tested for accuracy before

being used as input variables in the random forest model. The elevations computed from the 3D point clouds were compared with elevation values recorded with dGPS at each sampling quadrat point. The analysis yielded RMSE values between 5 cm for Tahu N and 18 cm for Hosby.

The contribution of each explanatory variable to the overall random forest model performance was assessed using percent increase in Mean Squared Error (MSE) test. The results of the predictor variables importance tests (Table 6) are very site-specific, although some trends can be observed. Digital terrain models show the highest contribution to the random forest model in Hosby, Matsalu 2, RumpoE and RumpoW. This result confirms the trend already highlighted by the RMSE and R² tests. Green Red Difference Index (GRDI) and some red-edge based indices (Red edge simple ratio (SRre), Red edge normalized difference vegetation index (NDVIre), DATT4) also contributed noticeably to the estimation of above-ground biomass.

3.2. Grassland sward structure

The Mean-Shift image segmentation procedure generated sward cluster maps corresponding to the nine study sites (Tahu S is shown in Fig. 4). Each individual cluster in the resulting maps represents a unit with homogeneous distribution and arrangement of above-ground biomass. Consequently, each cluster represents grassland structure heterogeneity in terms of distribution and size of vegetation patches and tussocks.

The results of the landscape index analysis at each study site are

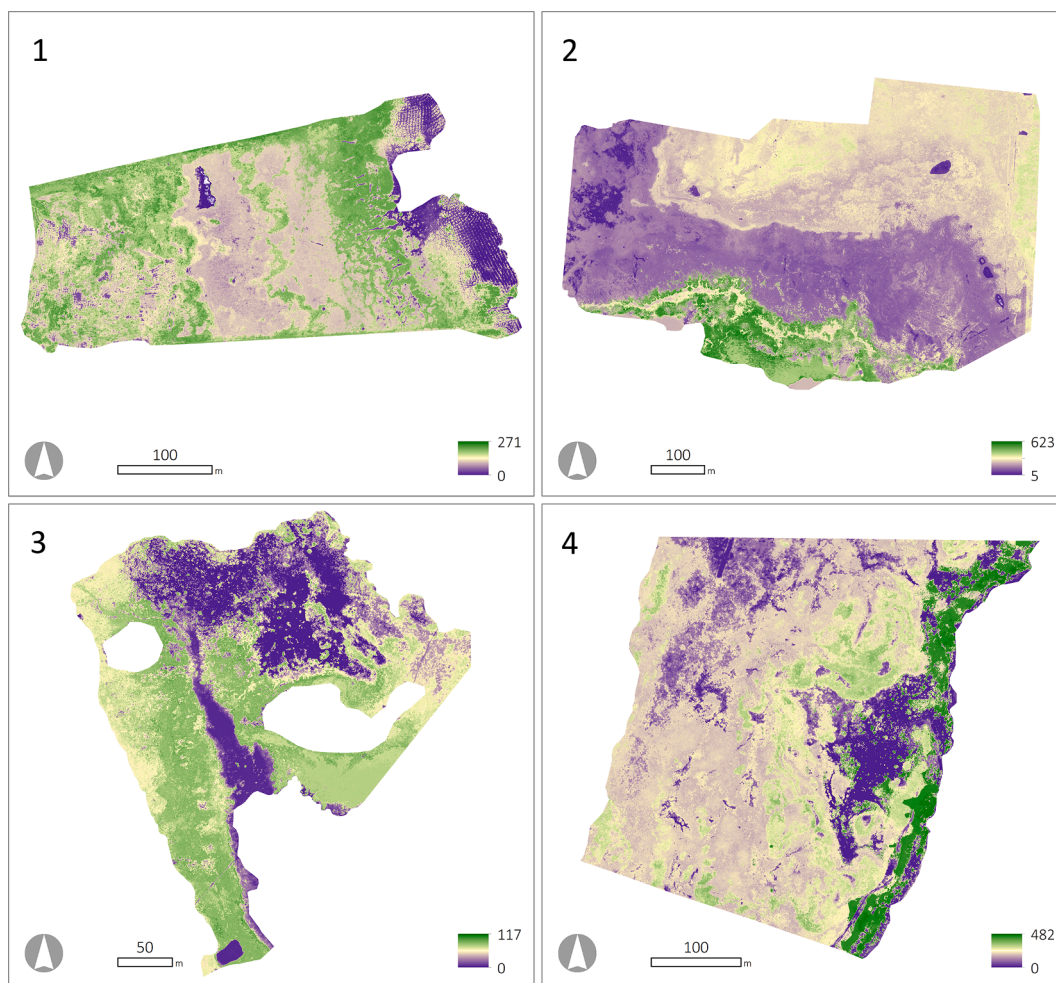


Fig. 3. Above-ground biomass predicted using a random forest algorithm with vegetation indices and SfM-derived microtopography. Four out of nine study sites are represented in this figure, 1: Tahu N; 2: Matsalu 2; 3: Rumpo E; 4: Hosby. All values are expressed as gr/m². Maps corresponding to all study sites are shown in Supplementary figures S1.

Table 5

RMSE and R² classification accuracies for predicted above-ground biomass at each study site. Prediction accuracies were calculated for two separate sets of explanatory variables: vegetation indices only and vegetation indices combined with SfM microtopography.

Test site	RMSE (gr/m ²)	R ²
Tahu N (Veg. indices)	24.48	0.9
Tahu N (Veg. indices + DTM)	26.24	0.9
Tahu S (Veg. indices)	35.12	0.89
Tahu S (Veg. indices + DTM)	31.76	0.91
Kudani (Veg. indices)	36.8	0.63
Kudani (Veg. indices + DTM)	34.57	0.849
Matsalu 1 (Veg. indices)	65.6	0.937
Matsalu 1 (Veg. indices + DTM)	57.44	0.95
Matsalu 2 (Veg. indices)	64.36	0.84
Matsalu 2 (Veg. indices + DTM)	47.29	0.91
Rälby (Veg. indices)	21.29	0.92
Rälby (Veg. indices + DTM)	-	-
Hosby (Veg. indices)	48.8	0.92
Hosby (Veg. indices + DTM)	24.2	0.981
Rumpo W (Veg. indices)	57.46	0.75
Rumpo W (Veg. indices + DTM)	43.57	0.861
Rumpo E (Veg. indices)	7.59	0.96
Rumpo E (Veg. indices + DTM)	6.2	0.975

presented in Table 7 and reflect the differences in sward complexity between sites. Large values of *largest patch index* and *patch average area* indicate structurally homogeneous and uniform swards, whereas large values of *patch density*, *edge density* and *landscape shape index* point out at complex and heterogeneous sward structures. Study sites in Silma Nature Reserve and Vormis Island show a higher degree of heterogeneity than those in Matsalu National Park, with very noticeable differences in largest patch index and patch density.

3.3. Effects of management on grassland structure

The GLM highlighted the effect of management type and history on

Table 6

Contribution of each variable to the overall performance of the Random Forest algorithm estimated by using percent increase in Mean Squared Error. Numbers represent the percent increase in mean squared error once a variable is permuted. Values below 5% are not represented in the table. Colour gradients represent the contribution of each variable to the overall performance.

	Hosby	Kudani	Matsalu 1	Matsalu 2	Rälby	RumpoE	Rumpo W	TahuN	TahuS
DTM	135.0	15.3	15.5	57.2	-	28.3	37.2	-	13.3
GRDI	72.9	14.2	19.5	17.0	27.0	14.8	9.1	9.2	20.1
DATT4	20.2	11.7	6.7	7.4	10.0	8.9	9.3	23.1	12.6
GDI	8.9	12.2	7.1	18.4	12.6	8.2	9.1	5.3	16.3
SRre	8.1	13.0	10.6	9.7	26.3	9.5	12.8	10.0	10.4
NDVlre	7.7	13.2	9.5	9.6	26.8	9.7	13.4	10.2	9.8
RTVlcore	5.1	14.7	9.1	8.4	8.6	12.6	8.6	8.0	15.4
NDVI	-	14.0	16.1	17.5	18.1	7.9	9.4	8.1	20.9
DVI	-	13.1	7.1	12.6	11.4	10.3	9.0	5.4	14.9
GNDVI	-	15.8	11.1	10.1	11.9	9.5	11.0	-	17.8
EVl2	-	11.1	5.6	9.2	11.4	8.8	10.6	9.8	12.3
GRVI	-	15.5	12.1	10.9	11.4	10.0	10.7	-	17.0
MSAVI	-	11.7	6.3	10.4	12.5	9.2	10.6	9.8	14.0
SAVI	-	11.3	5.9	9.4	12.0	9.0	11.3	9.2	12.7

Marginal
 Moderate
 High
 Very high

some landscape indices (Table 8). The number of years of uninterrupted grazing management had a significant positive effect ($p < 0.0001$) on patch average area and largest patch index, and a significant negative effect ($p < 0.0001$) on edge density, landscape shape index and patch density. These results indicate larger patches and grassland structure homogenization as the duration of management increases. Similarly, grazing management intensity had a significant positive ($p < 0.0001$) effect on largest patch index. Regarding livestock, the type of species present during the last two years had a significant effect on edge density, landscape shape index and largest patch index, whereas species present throughout the management history had a significant effect on edge density, largest patch index and edge density. No significant interactions were found between the management descriptors.

Mann-Whitney U tests further revealed the effects of livestock species on coastal meadow structure. The values for edge density, landscape shape index and patch density were significantly lower in cattle-grazed meadows than in those with a mixture of livestock throughout the management history ($p < 0.001$). Largest patch index and patch average area showed significantly higher values in cattle-grazed meadows than in those with a mixture of livestock during all management history ($p < 0.001$) (Fig. 5). No significant differences were found between cattle and horse grazed meadows during the last two years.

4. Discussion and conclusions

This study proposes a methodology to utilize UAVs as a tool to monitor the production of above-ground biomass (AGB) in coastal meadows and assess their structural complexity in relation to management history. In coastal meadows, management simultaneously drives the supply of multiple ecosystem services and affects the quality of habitat of wader species (Rhymer et al., 2010). As a result, conservation measures and agri-environmental schemes that target these valuable ecosystems must ensure the supply of ecosystem services whilst maintaining adequate habitat status. However, unveiling the complex balance between management, ecosystem structure, processes, functions

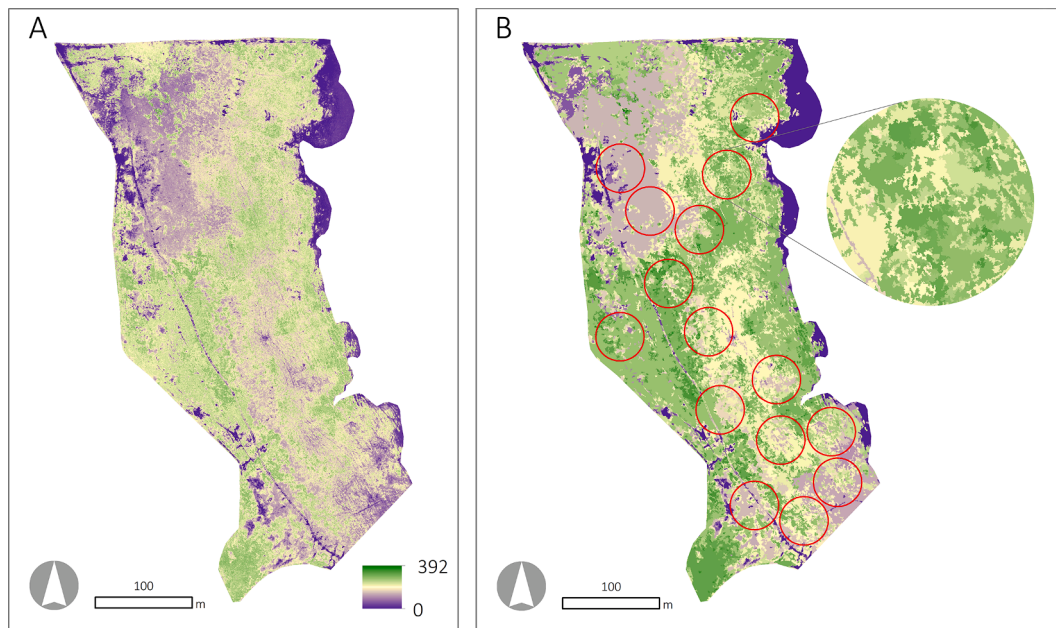


Fig. 4. Results of Mean-Shift image segmentation at Tahu S study site. “A” corresponds to the predicted above-ground biomass map whereas “B” shows the homogeneous biomass clusters. The red circles in “B” represent the sample units at which landscape indices were calculated. Values are expressed as gr/m². The results of the segmentation procedure in all study sites are presented in the Annex. (For interpretation of the references to colour in this figure legend, the reader is referred to the web version of this article.). Cluster maps corresponding to all study sites are shown in [Supplementary figures S2](#).

Table 7
Values of five landscape indices calculated at each study site.

Study site	Patch average area (m ²)	Patch density (nr patches*ha ⁻¹)	Edge density (m*ha ⁻¹)	Landscape shape index (unitless)	Largest patch index (%)
Tahu North	5.16	1937.86	9127.06	73.70	25.72
Tahu South	3.89	2569.58	12716.32	109.85	9.59
Kudani	4.91	2037.12	9092.50	125.97	13.06
Matsalu1	16.71	598.47	3114.61	39.30	80.97
Matsalu2	10.85	921.90	3716.48	59.94	77.94
Rumpo East	6.15	1625.79	9322.24	63.79	12.10
Rumpo West	5.42	1846.68	9630.13	41.89	14.61
Rälby	3.54	2825.67	10026.96	79.95	13.67
Hosby	7.47	1338.32	7610.38	76.32	33.85

and habitat quality requires timely and accurate spatially-explicit data (Bunce et al., 2008; Nagendra et al., 2013). In this regard, the emergence of UAVs as a tool for environmental monitoring (Ventura et al., 2017) has led to an unprecedented availability of data at ecologically relevant spatial and temporal scales (Pajares, 2015). These novel tools and datasets bring new opportunities for assessing and monitoring

Table 8
GLM analysis results (t and Pr(>|t|)) for the effects of management on grassland structure (landscape indices). Significance codes: p < 0.0001 “****”, p < 0.001 “***”, p < 0.01 “**”, p < 0,05 “+”. Only significant results are shown.

	Edge density		Landscape shape index		Patch density		Largest patch index		Patch average area	
	t value	Pr(> t)	t value	Pr(> t)	t value	Pr(> t)	t value	Pr(> t)	t value	Pr(> t)
Management duration	-8.203	3.79e-13 ***	-8.204	3.76e-13 ***	-5.993	2.42e-08 ***	8.410	1.27e-13 ***	5.747	7.58e-08 ***
Management intensity	-1.786	0.767 +					3.931	0.000145 ***		
Herbivore species (management history)	2.277	0.0246 *	1.705	0.0909 +	2.874	0.00483 **	-3.602	0.000468 ***	-1.868	0.0644 +
Herbivore species (last two years)	-2.450	0.0158 *	-2.019	0.0459 *			3.866	0.000184 ***		

ecosystem structure and functions, but entail high data volumes (Chi et al., 2016). This study demonstrates that UAVs can be coupled with plot-based vegetation surveys in order to reveal spatial patterns of coastal meadow structure and functions. However, further developments are needed in order to fully operationalize UAVs as monitoring tools.

4.1. High spatial resolution maps of standing above-ground biomass

A key aspect of the present study was the combination of multiple sensors in order to achieve reliable results. The Random Forest algorithm yielded better predictions of AGB when the combination of multispectral information with SfM-derived DTMs were used as explanatory variables. The increase in prediction accuracy is especially noticeable at the Hosby study site, where the RMSE shifted from 48.8 gr/m² to 24.2 gr/m². In coastal meadows, microtopography is strongly associated with soil moisture gradients, spatio-temporal fluctuations of flood levels and availability of nutrients (Ward et al., 2016a). These gradients, in turn, drive the distribution of plant communities in coastal wetlands (Ward et al., 2013) and the ecosystem functions underlying the supply of ecosystem services such as C sequestration, weathering processes and soil fertility, fodder for cattle and habitat for waders nursery and reproduction. The results achieved in this study suggest that combining multiple sensors enhances the capability to measure ecosystem characteristics that may be otherwise overlooked when relying solely on

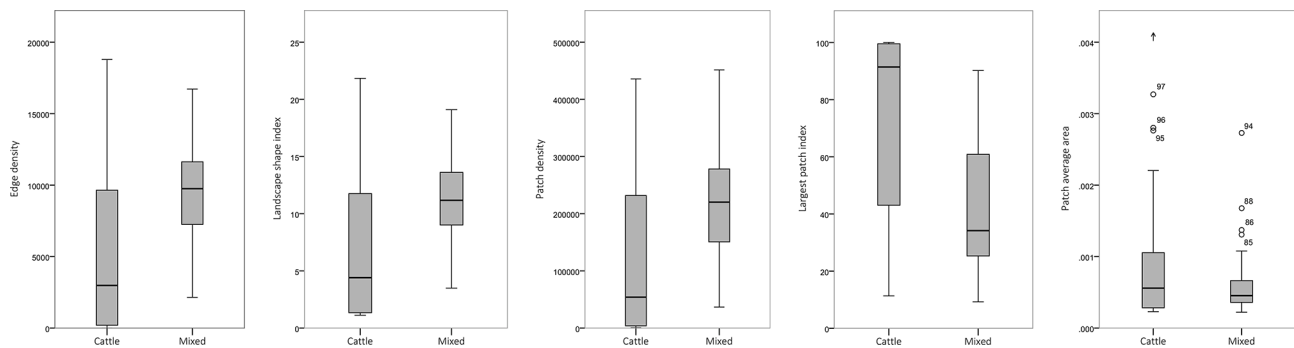


Fig. 5. Differences between the mean values of five landscape indices in cattle-grazed and mixed livestock-grazed grasslands. All differences were significant ($p < 0.001$). † indicates values out of the graph: 0.0654, 0.0981, 0.1962.

spectral information. Previous studies have shown that sensor fusion improves prediction and classification accuracies. For instance, Moeckel et al. (2017) improved the prediction accuracies of pasture biomass using a combination of data measured with ground-based ultrasonic distance sensors and spectral sensors. De Alban et al. (2018) combined Landsat multispectral data with L-band Synthetic Aperture Radar to enhance landuse/landcover change detection in tropical landscapes. Latifi et al. (2012) achieved improved models of above ground biomass and stem density in temperate forests in Germany using LiDAR metrics in combination with hyperspectral data. In the field of UAV remote sensing, some studies have used aerial photogrammetry (Zhang et al., 2018) or multispectral data (Grüner et al., 2020) to estimate grassland AGB, however only few have explored the possibilities of UAV-based sensor fusion to improve predictions.

Regarding prediction accuracies at different study sites, RMSE and R^2 values for predicted AGB ranged from 6.2 gr/m² in Rumpo E to 57.44 gr/m² in Matsalu1 and from 0.975 in Rumpo E to 0.85 in Kudani. These differences can be attributed to the characteristics of each study site in terms of plant communities and vegetation height. Very similar trends in modelling accuracies were found by Villoslada et al. (2020), where sites characterized by the presence of more productive communities or a higher herbage yield (such as Matsalu 1 and 2 in this study) show lower prediction accuracies than short-sward sites (such as Rumpo E, Tahu N and Tahu S in this study). It has been previously shown that the complexity of sward structures, vegetation height and plant species richness affect the spectral characteristics of training samples (Villoslada et al., 2020). This, in turn, has an effect on the overall prediction accuracy.

Together with overall accuracy estimations, predictor importance metrics provide a deeper insight into the performance of the random forest algorithm. The percent increase in MSE shows highly variable results between all study sites. However, within most site prediction models, DTMs exhibited a high prediction importance. These results are in accordance with the consistent increase in overall classification accuracy observed at most sites, with the exception of Tahu N, where DTM did not improve the model. The key role of remotely sensed micro-topographic data in the classification reinforces the idea that often, vegetation spectral information needs to be enhanced with ancillary data in order to obtain robust estimates (Sluiter and Pebesma, 2010). The Green-Red Difference Index (GRDI) also proved to be a relevant predictor. GRDI is known for its sensitivity to leaf density and its ability to predict the percentage of green herbage (Gianelle and Vescovo, 2007). The variability of results between sites reflects the wide range of characteristics at each site in terms of soil moisture, proportion of bare soil and vegetation height. These findings indicate that there is no optimal combination of vegetation indices or spectral bands when monitoring habitats at very detailed spatial resolutions. Using a wide spectrum of indices provides the flexibility needed to obtain robust results in variable environmental conditions.

4.2. Sward characterization

Based on the high spatial resolution biomass prediction maps, a grassland structure characterization was undertaken. A Mean-Shift segmentation routine was used to unveil sward structures from the continuous biomass data. Clustering techniques are commonly used to reveal vegetation structures and characteristics that remain otherwise hidden in continuous and multidimensional datasets (Kwak et al., 2010; Schirrmann et al., 2016). The Mean-Shift segmentation routine was chosen for its ability to process one-dimensional continuous data. The clustered data were analysed using five landscape indices, revealing distinct patterns of sward structure at each site. This clustering analysis and characterization constitutes a step forward in UAV-based vegetation assessments, as it expands the potential applications of UAVs towards ecosystem integrity and status assessments. Wetland and grassland habitats characterized by high spatial heterogeneity at micro scales can be surveyed following this approach, therefore expanding the scope of assessment beyond coastal meadows.

4.3. Effect of the duration and type of management regime

The potential linkages between sward structure data and management regime were analysed using a GLM, which highlighted the pivotal role of grazing intensity and duration on grassland heterogeneity. Uninterrupted grazing for longer periods resulted in meadows with larger and more homogeneous patches (higher values of largest patch index and patch average area and lower values of edge density, landscape shape index and patch density). This reveals the homogenizing effect that continuous, monospecific grazing may have on sward structure. In Estonian coastal meadows, cattle breeds have a limited selective grazing behaviour (Kuresoo and Mägi, 2004), which could lead to homogenization in the long term. This also suggests that grazing type, intensity and duration are likely to have an impact on rates of carbon sequestration through biomass inputs during seasonal dieback, as well as on total carbon stored, which is a suggested object of further study.

The effect of livestock species was also tested using GLM analysis and Mann-Whitney U tests. A mix of livestock species for management over time led to more structurally diverse coastal meadows than those grazed by cattle alone. This can be explained by the fact that different livestock species have different grazing behaviours that lead to distinct spatial and temporal grazing patterns (Loucougaray et al., 2004). Although bovines are regarded as suitable grazers for coastal meadow management (Kuresoo and Mägi, 2004), a mixture of livestock species may have additive effects on the structural characteristics of the meadow (Loucougaray et al., 2004), leading to more complex swards as opposed to monospecific grazing. Fine-tuning management strategies in coastal meadows is of key importance, as grassland structural characteristics and complexity are strongly associated with the nesting, breeding and foraging habitat quality for wader species (Smart et al., 2006). As an example, Common Redshank (*Tringa totanus*) prefers short grass areas

with patches of taller grass as breeding habitat (Rannap et al., 2017). Heterogeneous sward structures also widen the availability of microhabitats for invertebrates (Sanderson et al., 1995), which play an essential role in the supply of soil-related ecosystem services (Lavelle et al., 2006) such as nutrient cycling and carbon sequestration and storage.

4.4. UAVs as a tool for grassland monitoring

The approach presented in this study was successful in predicting AGB and characterizing sward complexity in relation to management, however, there are still certain methodological aspects that require improvement. Further research should directly couple UAV sward structure surveys with nest surveys in order to fully address the effects of sward structure in bird nesting and breeding success. Several UAV surveys should be conducted throughout the growing season to unveil the temporal dynamics of grassland sward complexity. Furthermore, UAV surveys are still constrained by flight duration and area coverage, thus limiting the areas to be monitored. In this regard, recent advances in the fusion of UAV and satellite data (Alvarez-Vanhard et al., 2020) set a promising path towards remote sensing-based monitoring.

The results achieved in this study demonstrate the use of UAVs in coastal meadow monitoring. The multifunctional role of coastal meadows as suppliers of a range of ecosystem services for society (e.g. sediment trapping, carbon sequestration, nutrient recycling, reared animals, pollination, habitat for waders) depends upon balanced site-specific management strategies. Continuous biomass monitoring with UAVs can support tailored management options aimed at finding optimal balances between livestock production, carbon sequestration and accumulation, and habitat conservation. In this regard, sensor fusion and a broad range of remotely sensed predictor variables ensure higher prediction accuracies and adaptability to study site conditions.

This study also sets the path to UAV-based assessments of ecosystem services supply and blue carbon sequestration estimations. Future research should explore the use of UAV-based data to quantify a broader range of habitat quality parameters in coastal meadows as well as explore the use of UAV-based data and machine learning algorithm techniques to evaluate carbon storage. Specifically in coastal meadows, the accuracy of estimations of carbon stocks and storage rates directly depends on accurate quantifications of the spatial variation of above-ground biomass (Owers et al., 2018).

CRedit authorship contribution statement

M. Villoslada Pecina: Conceptualization, Methodology, Data curation. **T.F. Bergamo:** Conceptualization, Methodology, Data curation. **R. D. Ward:** Conceptualization, Methodology. **C.B. Joyce:** Conceptualization. **K. Sepp:** Supervision.

Declaration of Competing Interest

The authors declare that they have no known competing financial interests or personal relationships that could have appeared to influence the work reported in this paper.

Acknowledgements

This study has been supported by the EU Mobilitas Plus Researcher Grant MOBJD243 and by the European Regional Development Fund within the Estonian National Programme for Addressing Socio-Economic Challenges through R&D (RITA) (Estonia). The authors thank Kaja Lotman and Elle Puurmann for conducting interviews with land owners to obtain management information for the studied sites. The authors would also like to thank Kaja Orupõld for her support and collaboration.

Appendix A. Supplementary data

Supplementary data to this article can be found online at <https://doi.org/10.1016/j.ecolind.2020.107227>.

References

- Adão, T., Hruška, J., Pádua, L., Bessa, J., Peres, E., Morais, R., Sousa, J., 2017. Hyperspectral imaging: a review on UAV-based sensors, data processing and applications for agriculture and forestry. *Remote Sens.* 9 (11), 1110. <https://doi.org/10.3390/rs9111110>.
- Akumu, C.E., Pathirana, S., Baban, S., Bucher, D., 2010. Monitoring coastal wetland communities in north-eastern NSW using ASTER and Landsat satellite data. *Wetlands Ecol. Manage.* 18 (3), 357–365. <https://doi.org/10.1007/s11273-010-9176-0>.
- Aldabe, J., Lancot, R.B., Blanco, D., Rocca, P., Inchausti, P., 2019. Managing grasslands to maximize migratory shorebird use and livestock production. *Rangeland Ecol. Manage.* 72 (1), 150–159. <https://doi.org/10.1016/j.rama.2018.08.001>.
- Ali, I., Cawkwell, F., Dwyer, E., Barrett, B., Green, S., 2016. Satellite remote sensing of grasslands: from observation to management. *J. Plant Ecol.* 9 (6), 649–671. <https://doi.org/10.1093/jpe/rtw005>.
- Alvarez-Vanhard, E., Houet, T., Mony, C., Lecoq, L., Corpetti, T., 2020. Can UAVs fill the gap between in situ surveys and satellites for habitat mapping? *Remote Sens. Environ.* 243, 111780. <https://doi.org/10.1016/j.rse.2020.111780>.
- Baena, S., Boyd, D.S., Moat, J., 2018. UAVs in pursuit of plant conservation - real world experiences. *Ecol. Inf.* 47, 2–9. <https://doi.org/10.1016/j.ecoinf.2017.11.001>.
- Baena, S., Moat, J., Whaley, O., Boyd, D.S., 2017. Identifying species from the air: UAVs and the very high resolution challenge for plant conservation. *Plos One* 12 (11). <https://doi.org/10.1371/journal.pone.0188714>.
- Barbier, E., 2013. Valuing ecosystem services for coastal wetland protection and restoration: progress and challenges. *Resources* 2 (3), 213–230. <https://doi.org/10.3390/resources2030213>.
- Barbier, E.B., Hacker, S.D., Kennedy, C., Koch, E.W., Stier, A.C., Silliman, B.R., 2011. The value of estuarine and coastal ecosystem services. *Ecol. Monogr.* 81 (2), 169–193. <https://doi.org/10.1890/10.1890/10-1510.1>.
- Baxter, P.W.J., Hamilton, G., 2018. Learning to fly: integrating spatial ecology with unmanned aerial vehicle surveys. *Ecosphere* 9 (4). <https://doi.org/10.1002/ecs2.2194>.
- Berg, M., Joyce, C., Burnside, N., 2012. Differential responses of abandoned wet grassland plant communities to reinstated cutting management. *Hydrobiologia* 692 (1), 83–97. <https://doi.org/10.1007/s10750-011-0826-x>.
- Breiman, L., 2001. Random forests. *Mach. Learn.* 45 (1), 5–32. <https://doi.org/10.1023/A:1010933404324>.
- Bunce, R.G.H., Metzger, M.J., Jongman, R.H.G., Brandt, J., de Blust, G., Elena-Rossello, R., Groom, G.B., Halada, L., Hofer, G., Howard, D.C., Kovár, P., Múcher, C. A., Padoa-Schioppa, E., Paelinx, D., Palo, A., Perez-Soba, M., Ramos, I.L., Roche, P., Skånes, H., Wrba, T., 2008. A standardized procedure for surveillance and monitoring European habitats and provision of spatial data. *Landscape Ecol.* 23 (1), 11–25. <https://doi.org/10.1007/s10980-007-9173-8>.
- Burnside, N.G., Joyce, C.B., Puurmann, E., Scott, D.M., 2007. Use of vegetation classification and plant indicators to assess grazing abandonment in Estonian wet grasslands. *J. Veg. Sci.* 18, 645–654. <https://doi.org/10.1111/j.1654-1103.2007.tb02578.x>.
- Chi, M., Plaza, A., Benediktsson, J.A., Sun, Z., Shen, J., Zhu, Y., 2016. Big data for remote sensing: challenges and opportunities. *Proc. IEEE* 104 (11). <https://doi.org/10.1109/jproc.2016.2598228>.
- Clausen, K.K., Stjernholm, M., Clausen, P., 2013. Grazing management can counteract the impacts of climate change-induced sea level rise on salt marsh-dependent waterbirds. *J. Appl. Ecol.* 50 (2), 528–537. <https://doi.org/10.1111/1365-2664.12043>.
- Comaniciu, D., Meer, P., 2002. Mean shift: a robust approach toward feature space analysis. *IEEE Trans. Pattern Anal. Mach. Intell.* 24 (5), 603–619. <https://doi.org/10.1109/34.1000236>.
- Datt, B., 1998. Remote sensing of chlorophyll a, chlorophyll b, chlorophyll a b, and Total Carotenoid Content in Eucalyptus Leaves. *Remote Sens. Environ.* 66 (2), 111–121. [https://doi.org/10.1016/s0034-4257\(98\)00046-7](https://doi.org/10.1016/s0034-4257(98)00046-7).
- De Alban, J.D.T., Connette, G.M., Oswald, P., Webb, E.L., 2018. Combined Landsat and L-band SAR data improves land cover classification and change detection in dynamic tropical landscapes. *Remote Sens.* 10 (2), 306. <https://doi.org/10.3390/rs10020306>.
- Díaz-Delgado, R., Cazacu, C., Adamescu, M., 2018. Rapid assessment of ecological integrity for LTER wetland sites by using UAV multispectral mapping. *Drones* 3 (1), 3. <https://doi.org/10.3390/drones3010003>.
- Doughty, C., Cavanaugh, K., 2019. Mapping coastal wetland biomass from high resolution unmanned aerial vehicle (UAV) imagery. *Remote Sens.* 11 (5), 540. <https://doi.org/10.3390/rs11050540>.
- Duarte, C.M., Losada, I.J., Hendriks, I.E., Mazarrasa, I., Marbà, N., 2013. The role of coastal plant communities for climate change mitigation and adaptation. *Nat. Clim. Change* 3 (11), 961–968. <https://doi.org/10.1038/nclimate1970>.
- Enríquez, S., Duarte, C.M., Sand-Jensen, K., 1993. Patterns in decomposition rates among photosynthetic organisms: the importance of detritus C:N:P content. *Oecologia* 94 (4), 457–471. <https://doi.org/10.1007/BF00566960>.
- Guerini Filho, M., Kuplich, T.M., Quadros, F.L.F.D., 2020. Estimating natural grassland biomass by vegetation indices using Sentinel 2 remote sensing data. *Int. J. Remote Sens.* 41 (8), 2861–2876. <https://doi.org/10.1080/01431161.2019.1697004>.

- Freeman, E., Frescino, T., Moisen, G., 2009. ModelMap: An R Package for Modeling and Map Production Using Random Forest and Stochastic Gradient Boosting. USDA Forest Service, Rocky Mountain Research, Station, p. 507.
- Gianelle, D., Vescovo, L., 2007. Determination of green herbage ratio in grasslands usingspectral reflectance. Methods and ground measurements. *Int. J. Remote Sens.* 28 (5), 931–942. <https://doi.org/10.1080/0143116050019639>.
- Giri, C., Ochieng, E., Tieszen, L.L., Zhu, Z., Singh, A., Loveland, T., et al., 2010. Status and distribution of mangrove forests of the world using earth observation satellite data. *Global Ecol. Biogeogr.* 20 (1), 154–159. <https://doi.org/10.1111/j.1466-8238.2010.00584.x>.
- Gitelson, A.A., Kaufman, Y.J., Merzlyak, M.N., 1996. Use of a green channel in remote sensing of global vegetation from EOS-MODIS. *Remote Sens. Environ.* 58 (3), 289–298. [https://doi.org/10.1016/S0034-4257\(96\)00072-7](https://doi.org/10.1016/S0034-4257(96)00072-7).
- Gitelson, A., Merzlyak, M.N., 1994. Spectral reflectance changes associated with autumn senescence of *Aesculus hippocastanum* L. and *Acer platanoides* L. Leaves. Spectral features and relation to chlorophyll estimation. *J. Plant Physiol.* 143 (3), 286–292. [https://doi.org/10.1016/S0176-1617\(11\)81633-0](https://doi.org/10.1016/S0176-1617(11)81633-0).
- Grüner, E., Wachendorf, M., Astor, T., 2020. The potential of UAV-borne spectral and textural information for predicting aboveground biomass and N fixation in legume-grass mixtures. *Plos One* 15 (6). <https://doi.org/10.1371/journal.pone.0234703>.
- Haines-Young, R., Potschin, M.B., 2018. Common international Classification of Ecosystem Services (CICES) V5. Fabis Consulting Ltd., Nottingham, UK.
- Henle, K., Alard, D., Clitherow, J., Cobb, P., Firbank, L., Kull, T., McCracken, D., Moritz, R.F.A., Niemelä, J., Rebane, M., Wascher, D., Watt, A., Young, J., 2008. Identifying and managing the conflicts between agriculture and biodiversity conservation in Europe—a review. *Agric. Ecosyst. Environ.* 124 (1–2), 60–71. <https://doi.org/10.1016/j.agee.2007.09.005>.
- Hesselbarth, M.H.K., Sciaini, M., With, K.A., Wiegand, K., Nowosad, J., 2019. landscapemetrics: an open-source R tool to calculate landscape metrics. *Ecography* 42 (10), 1648–1657. <https://doi.org/10.1111/ecog.04617>.
- Hijmans, R.J., van Etten, J., 2012. Raster: Geographic analysis and modeling with raster data. R package version 2.0-12. <http://CRAN.R-project.org/package=raster>.
- Huete, A.R., 1988. A soil-adjusted vegetation index (SAVI). *Remote Sens. Environ.* 25 (3), 295–309. [https://doi.org/10.1016/0034-4257\(88\)90106-X](https://doi.org/10.1016/0034-4257(88)90106-X).
- Jiang, Z., Huete, A.R., Didan, K., Miura, T., 2008. Development of a two-band enhanced vegetation index without a blue band. *Remote Sens. Environ.* 112 (10), 3833–3845. <https://doi.org/10.1016/j.rse.2008.06.006>.
- Jing, Y., Yang, X., Qiu, J., Li, J., Gao, T., Wu, Q., et al., 2014. Remote Sensing-Based Biomass Estimation and Its Spatio-Temporal Variations in Temperate Grassland, Northern China. *Remote Sens.* 6 (2), 1496–1513. <https://doi.org/10.3390/rs6021496>.
- Joyce, C., Simpson, M., Casanova, M., 2016. Future wet grasslands: ecological implications of climate change. *Ecosyst. Health Sustainability* 2 (9), 1–15. <https://doi.org/10.1002/ehs2.1240>.
- Kalacska, M., Chmura, G.L., Lucanus, O., Bérubé, D., Arroyo-Mora, J.P., 2017. Structure from motion will revolutionize analyses of tidal wetland landscapes. *Remote Sens. Environ.* 199, 14–24. <https://doi.org/10.1016/j.rse.2017.06.023>.
- Kont, A., Jaagus, J., Aunap, R., 2003. Climate change scenarios and the effect of sea-level rise for Estonia. *Global Planet. Change* 36 (1–2), 1–15. [https://doi.org/10.1016/S0921-8181\(02\)00149-2](https://doi.org/10.1016/S0921-8181(02)00149-2).
- Kross, A., McNairn, H., Lapen, D., Sunohara, M., Champagne, C., 2015. Assessment of RapidEye vegetation indices for estimation of leaf area index and biomass in corn and soybean crops. *Int. J. Appl. Earth Obs. Geoinf.* 34, 235–248. <https://doi.org/10.1016/j.jag.2014.08.002>.
- Kumar, L., Sinha, P., 2014. Mapping salt-marsh land-cover vegetation using high-spatial and hyperspectral satellite data to assist wetland inventory. *GIScience Remote Sens.* 51 (5), 483–497. <https://doi.org/10.1080/15481603.2014.947838>.
- Kuresoo, A., Mägi, E., 2004. Changes of bird communities in relation to management of coastal meadows in Estonia. In: Rannap, R., Briggs, L., Lotman, K., Lepik, I., Rannap, V., Põdra, P. (Eds.), *Coastal Meadow Management: Best Practice Guidelines*, pp. 52–61.
- Kwak, D.-A., Lee, W.-K., Cho, H.-K., Lee, S.-H., Son, Y., Kafatos, M., Kim, S.-R., 2010. Estimating stem volume and biomass of *Pinus koraiensis* using LiDAR data. *J. Plant. Res.* 123 (4), 421–432. <https://doi.org/10.1007/s10265-010-0310-0>.
- Laca, E. A., Lemaire, Z., 2000. Measuring Sward Structure 5. Field and laboratory methods for grassland and animal production research, 103.
- Lary, D.J., Alavi, A.H., Gandomi, A.H., Walker, A.L., 2016. Machine learning in geosciences and remote sensing. *Geosci. Front.* 7 (1), 3–10. <https://doi.org/10.1016/j.gsf.2015.07.003>.
- Latifi, H., Fassnacht, F., Koch, B., 2012. Forest structure modeling with combined airborne hyperspectral and LiDAR data. *Remote Sens. Environ.* 121, 10–25. <https://doi.org/10.1109/igars.2016.7729922>.
- Lavelle, P., Decaëns, T., Aubert, M., Barot, S., Blouin, M., Bureau, F., Rossi, J.P., 2006. Soil invertebrates and ecosystem services. *Eur. J. Soil Biol.* 42, S3–S15. <https://doi.org/10.1016/j.ejsobi.2006.10.002>.
- Leito, A., Elts, J., Mägi, E., Ivask, I., Ööpik, M., Sepp, K., Ward, R., 2014. Coastal grassland wader abundance in relation to breeding habitat characteristics and prey abundance in Matsalu. *Estonia Ornithologica* 91, 149–165.
- Liaw, A., Wiener, M., 2002. Classification and Regression by random Forest. *R News* 2 (3), 18–22. <http://cran.r-project.org/web/packages/randomForest>.
- Lima, M., Ward, R., Joyce, C., 2020. Environmental drivers of carbon stocks in temperate seagrass meadows. *Hydrobiologia*. <https://doi.org/10.1007/s10750-019-04153-5>.
- Loucougaray, G., Bonis, A., Bouzillé, J.-B., 2004. Effects of grazing by horses and/or cattle on the diversity of coastal grasslands in western France. *Biol. Conserv.* 116 (1), 59–71. [https://doi.org/10.1016/S0006-3207\(03\)00177-0](https://doi.org/10.1016/S0006-3207(03)00177-0).
- López, J.J., Mulero-Pázmány, M., 2019. Drones for conservation in protected areas: present and future. *Drones* 3 (1), 10. <https://doi.org/10.3390/drones3010010>.
- Mafi-Gholami, D., Zenner, E.K., Jaafari, A., Ward, R.D., 2018. Modeling multi-decadal mangrove leaf area index in response to drought along the semi-arid southern coasts of Iran. *Sci. Total Environ.* 656, 1326–1336. <https://doi.org/10.1016/j.scitotenv.2018.11.462>.
- Maguigan, M., Rodgers, J., Dash, P., Meng, Q., 2016. Assessing net primary production in montane wetlands from proximal, airborne, and satellite remote sensing. *Adv. Remote Sens.* 05 (02), 118–130. <https://doi.org/10.4236/ars.2016.52010>.
- Martin, C.L., Momtaz, S., Gaston, T., Moltchanivskiy, N.A., 2016. A systematic quantitative review of coastal and marine cultural ecosystem services: current status and future research. *Mar. Policy* 74, 25–32. <https://doi.org/10.1016/j.marpol.2016.09.004>.
- Martin, F., Müllerová, J., Borgniet, L., Dommanget, F., Breton, V., Evette, A., 2018. Using single- and multi-date UAV and satellite imagery to accurately monitor invasive knotted species. *Remote Sens.* 10 (10), 1662. <https://doi.org/10.3390/rs10101662>.
- Mcleod, E., Chmura, G.L., Bouillon, S., Salm, R., Björk, M., Duarte, C.M., et al., 2011. A blueprint for blue carbon: toward an improved understanding of the role of vegetated coastal habitats in sequestering CO₂. *Front. Ecol. Environ.* 9 (10), 552–560. <https://doi.org/10.1890/110004>.
- Meng, X., Shang, N., Zhang, X., Li, C., Zhao, K., Qiu, X., Weeks, E., 2017. Photogrammetric UAV mapping of terrain under dense coastal vegetation: an object-oriented classification ensemble algorithm for classification and terrain correction. *Remote Sens.* 9 (11), 1187. <https://doi.org/10.3390/rs9111187>.
- Moekkel, T., Safari, H., Reddersen, B., Fricke, T., Wachendorf, M., 2017. Fusion of ultrasonic and spectral sensor data for improving the estimation of biomass in grasslands with heterogeneous sward structure. *Remote Sens.* 9 (1), 98. <https://doi.org/10.3390/rs9010098>.
- Mutanga Correspond, O., Skidmore, A.K., 2004. Narrow band vegetation indices overcome the saturation problem in biomass estimation. *Int. J. Remote Sens.* 25 (19), 3999–4014. <https://doi.org/10.1080/01431160310001654923>.
- Mutanga, O., Adam, E., Cho, M.A., 2012. High density biomass estimation for wetland vegetation using WorldView-2 imagery and random forest regression algorithm. *Int. J. Appl. Earth Obs. Geoinf.* 18, 399–406. <https://doi.org/10.1016/j.jag.2012.03.012>.
- Nagendra, H., Lucas, R., Honrado, J.P., Jongman, R.H.G., Tarantino, C., Adamo, M., Mairota, P., 2013. Remote sensing for conservation monitoring: assessing protected areas, habitat extent, habitat condition, species diversity, and threats. *Ecol. Ind.* 33, 45–59. <https://doi.org/10.1016/j.ecolind.2012.09.014>.
- Naidoo, L., van Deventer, H., Ramoelo, A., Mathieu, R., Nondlazi, B., Gangat, R., 2019. Estimating above ground biomass as an indicator of carbon storage in vegetated wetlands of the grassland biome of South Africa. *Int. J. Appl. Earth Obs. Geoinf.* 78, 118–129. <https://doi.org/10.1016/j.jag.2019.01.021>.
- Nolte, S., Esselink, P., Smit, C., Bakker, J.P., 2014. Herbivore species and density affect vegetation-structure patchiness in salt marshes. *Agric. Ecosyst. Environ.* 185, 41–47. <https://doi.org/10.1016/j.agee.2013.12.010>.
- O'Donnell, J., Schalles, J., 2016. Examination of abiotic drivers and their influence on spartina alterniflora biomass over a twenty-eight year period using Landsat 5 TM satellite imagery of the Central Georgia Coast. *Remote Sens.* 8 (6), 477. <https://doi.org/10.3390/rs8060477>.
- Olsen, Y.S., Dausse, A., Garbutt, A., Ford, H., Thomas, D.N., Jones, D.L., 2011. Cattle grazing drives nitrogen and carbon cycling in a temperate salt marsh. *Soil Biol. Biochem.* 43 (3), 531–541. <https://doi.org/10.1016/j.soilbio.2010.11.018>.
- Owers, C.J., Rogers, K., Woodroffe, C.D., 2018. Spatial variation of above-ground carbon storage in temperate coastal wetlands. *Estuar. Coast. Shelf Sci.* 210, 55–67. <https://doi.org/10.1016/j.ecss.2018.06.002>.
- Pajares, G., 2015. Overview and current status of remote sensing applications based on unmanned aerial vehicles (UAVs). *Photogram Engng Rem Sens* 81 (4), 281–330. <https://doi.org/10.14358/PERS.81.4.281>.
- Palm, V., Sepp, M., Truu, J., Ward, R., Leito, A., 2017. The effect of atmospheric circulation on spring arrival of short- and long-distance migratory bird species in Estonia. *Boreal Environ. Res.* 22, 97–114.
- Plexida, S.G., Sfougaris, A.I., Ispikoudis, I.P., Papanastasis, V.P., 2014. Selecting landscape metrics as indicators of spatial heterogeneity—a comparison among Greek landscapes. *Int. J. Appl. Earth Obs. Geoinf.* 26, 26–35. <https://doi.org/10.1016/j.jag.2013.05.001>.
- Qui, J., Chehbouni, A., Huete, A.R., Kerr, Y.H., Sorooshian, S., 1994. A modified soil adjusted vegetation index. *Remote Sens. Environ.* 48 (2), 119–126. [https://doi.org/10.1016/0034-4257\(94\)90134-1](https://doi.org/10.1016/0034-4257(94)90134-1).
- Rannap, R., Kaart, T., Pehlak, H., Kana, S., Soomets, E., Lanno, K., 2017. Coastal meadow management for threatened waders has a strong supporting impact on meadow plants and amphibians. *J. Nat. Conserv.* 35, 77–91. <https://doi.org/10.1016/j.jnc.2016.12.004>.
- Ren, H., Zhou, G., Zhang, X., 2011. Estimation of green aboveground biomass of desert steppe in Inner Mongolia based on red-edge reflectance curve area method. *Biosyst. Eng.* 109 (4), 385–395. <https://doi.org/10.1016/j.biosystemseng.2011.05.004>.
- Rhymer, C.M., Robinson, R.A., Smart, J., Whittingham, M.J., 2010. Can ecosystem services be integrated with conservation? A case study of breeding waders on grassland. *Ibis* 152 (4), 698–712. <https://doi.org/10.1111/j.1474-919X.2010.01049.x>.
- Richardson, A.J., Everitt, J.H., 1992. Using spectral vegetation indices to estimate rangeland productivity. *Geocarto Int.* 7 (1), 63–69. <https://doi.org/10.1080/10106049209354353>.
- Rivis, R., Kont, A., Ratas, U., Palginömm, V., Antso, K., Tõnisson, H., 2016. Trends in the development of Estonian coastal land cover and landscapes caused by natural

- changes and human impact. *J. Coastal Conserv.* 20 (3), 199–209. <https://doi.org/10.1007/s11852-016-0430-3>.
- Rouse, J.W., Haas, R.H., Schell, J.A., Deering, D.W., 1974. Monitoring vegetation systems in the Great Plains with ERTS. *NASA Spec. Publ.* 351, 309.
- Salomidi, M., Katsanevakis, S., Borja, A., Braeckman, U., Damalas, D., Galparsoro, I., et al., 2012. Assessment of goods and services, vulnerability, and conservation status of European seabed biotopes: a stepping stone towards ecosystem-based marine spatial management. *Mediterr. Mar. Sci.* 13 (1), 49. <https://doi.org/10.12681/mms.23>.
- Sanderson, R.A., Rushton, S.P., Cherrill, A.J., Byrne, J.P., 1995. Soil, vegetation and space: an analysis of their effects on the invertebrate communities of a Moorland in North-East England. *J. Appl. Ecol.* 32 (3), 506. <https://doi.org/10.2307/2404648>.
- Schirrmann, M., Hamdorf, A., Garz, A., Ustyuzhanin, A., Dammer, K.-H., 2016. Estimating wheat biomass by combining image clustering with crop height. *Comput. Electron. Agric.* 121, 374–384. <https://doi.org/10.1016/j.compag.2016.01.007>.
- Sharps, E., Garbutt, A., Hiddink, J.G., Smart, J., Skov, M.W., 2016. Light grazing of saltmarshes increases the availability of nest sites for Common Redshank *Tringa totanus*, but reduces their quality. *Agric. Ecosyst. Environ.* 221, 71–78. <https://doi.org/10.1016/j.agee.2016.01.030>.
- Sing, T., Sander, O., Beerenwinkel, N., Lengauer, T., 2005. ROCR: visualizing classifier performance in R. *Bioinformatics* 21 (20), 7881. <https://cran.r-project.org/web/packages/ROCR/>.
- Sluiter, R., Pebesma, E.J., 2010. Comparing techniques for vegetation classification using multi- and hyperspectral images and ancillary environmental data. *Int. J. Remote Sens.* 31 (23), 6143–6161. <https://doi.org/10.1080/01431160903401379>.
- Smart, J., Gill, J.A., Sutherland, W.J., Watkinson, A.R., 2006. Grassland-breeding waders: identifying key habitat requirements for management. *J. Appl. Ecol.* 43 (3), 454–463. <https://doi.org/10.1111/j.1365-2664.2006.01166.x>.
- Smith, M.W., Carrivick, J.L., Quincey, D.J., 2015. Structure from motion photogrammetry in physical geography. *Prog. Phys. Geogr.: Earth Environ.* 40 (2), 247–275. <https://doi.org/10.1177/03091333155615805>.
- Spalding, M.D., Ruffo, S., Lacambra, C., Meliane, I., Hale, L.Z., Shepard, C.C., Beck, M. W., 2014. The role of ecosystems in coastal protection: Adapting to climate change and coastal hazards. *Ocean Coast. Manag.* 90, 50–57. <https://doi.org/10.1016/j.ocecoaman.2013.09.007>.
- Sripada, R.P., Heiniger, R.W., White, J.G., Meijer, A.D., 2006. Aerial color infrared photography for determining early in-season nitrogen requirements in corn. *Agron. J.* 98 (4), 968–977. <https://doi.org/10.2134/agronj2005.0200>.
- Summers, R.W., Stansfield, J., Perry, S., Atkins, C., Bishop, J., 1993. Utilization, diet and diet selection by brent geese *Branta bernicla bernicla* salt-marshes in Norfolk. *J. Zool.* 231 (2), 249–273. <https://doi.org/10.1111/j.1469-7998.1993.tb01916.x>.
- Suursaar, Ü., Sooäär, J., 2007. Decadal variations in mean and extreme sea level values along the Estonian coast of the Baltic Sea. *Tellus A: Dynamic Meteorol. Oceanogr.* 59 (2), 249–260. <https://doi.org/10.1111/j.1600-0870.2006.00220.x>.
- Taddia, Y., Nardin, W., Corbau, C., Franchi, G., Stevenson, C.J., Staver, L.W., 2019. Channels' shape evolution detected by uavs in a restored salt marsh. *Coastal Sediments 2019*. https://doi.org/10.1142/9789811204487_0131.
- Tadrowski, T., 2014. Accurate mapping using drones (UAV's). *Geoinformatics* 17 (8), 18.
- Thorne, K.M., Takekawa, J.Y., Elliott-Fisk, D.L., 2012. Ecological effects of climate change on salt marsh wildlife: a case study from a highly urbanized estuary. *J. Coastal Res.* 285, 1477–1487. <https://doi.org/10.2112/JCOASTRES-D-11-00136.1>.
- Tichit, M., Durant, D., Kernéis, E., 2005. The role of grazing in creating suitable sward structures for breeding waders in agricultural landscapes. *Livestock Prod. Sci.* 96 (1), 119–128. <https://doi.org/10.1016/j.livprodsci.2005.05.010>.
- Torma, A., Császár, P., Bozsó, M., Deák, B., Valkó, O., Kiss, O., Gallé, R., 2019. Species and functional diversity of arthropod assemblages (Araneae, Carabidae, Heteroptera and Orthoptera) in grazed and mown salt grasslands. *Agric. Ecosyst. Environ.* 273, 70–79. <https://doi.org/10.1016/j.agee.2018.12.004>.
- Ullah, S., Si, Y., Schlerf, M., Skidmore, A.K., Shafique, M., Iqbal, I.A., 2012. Estimation of grassland biomass and nitrogen using MERIS data. *Int. J. Appl. Earth Obs. Geoinf.* 19, 196–204. <https://doi.org/10.1016/j.jag.2012.05.008>.
- Veettil, B.K., Ward, R.D., Lima, M.D.A.C., Stankovic, M., Hoai, P.N., Quang, N.X., 2020. Opportunities for seagrass research derived from remote sensing: a review of current methods. *Ecol. Ind.* 117, 106560. <https://doi.org/10.1016/j.ecolind.2020.106560>.
- Ventura, D., Bonifazi, A., Gravina, M.F., Ardizzone, G.D., 2017. Unmanned aerial systems (UASs) for environmental monitoring: a review with applications in coastal habitats. *Aerial Robots-Aerodyn., Control Appl.* 165–184. <https://doi.org/10.5772/intechopen.69598>.
- Verhulst, J., Kleijn, D., Loonen, W., Berendse, F., Smit, C., 2011. Seasonal distribution of meadow birds in relation to in-field heterogeneity and management. *Agric. Ecosyst. Environ.* 142 (3–4), 161–166. <https://doi.org/10.1016/j.agee.2011.04.016>.
- Vihervaara, P., Auvinen, A.-P., Mononen, L., Törmä, M., Ahlroth, P., Anttila, S., Böttcher, K., Forsius, M., Heino, J., Heliölä, J., Koskelainen, M., Kuussaari, M., Meissner, K., Ojala, O., Tuominen, S., Viitasalo, M., Virkkala, R., 2017. How Essential Biodiversity Variables and remote sensing can help national biodiversity monitoring. *Global Ecol. Conserv.* 10, 43–59. <https://doi.org/10.1016/j.gecco.2017.01.007>.
- Villoslada, M., Bergamo, T.F., Ward, R.D., Burnside, N.G., Joyce, C.B., Bunce, R.G.H., Sepp, K., 2020. Fine scale plant community assessment in coastal meadows using UAV based multispectral data. *Ecol. Ind.* 111, 105979. <https://doi.org/10.1016/j.ecolind.2019.105979>.
- Vulink, J.T., van Eerden, M.R., Drent, R.H., 2010. Abundance of migratory and wintering geese in relation to vegetation succession in man-made wetlands: the effects of grazing regimes. *Ardea* 98 (3), 319–327. <https://doi.org/10.5253/078.098.0306>.
- Ward, R.D., 2020a. Carbon sequestration and storage in Norwegian Arctic coastal wetlands: Impacts of climate change. *Sci. Total Environ.* 748, 141343. <https://doi.org/10.1016/j.scitotenv.2020.141343>.
- Ward, R.D., 2020b. Sedimentary response of Arctic coastal wetlands to sea level rise. *Geomorphology* 370, 107400. <https://doi.org/10.1016/j.geomorph.2020.107400>.
- Ward, R.D., Burnside, N.G., Joyce, C.B., Sepp, K., 2013. The use of medium point density LiDAR elevation data to determine plant community types in Baltic coastal wetlands. *Ecol. Ind.* 33, 96–104. <https://doi.org/10.1016/j.ecolind.2012.08.016>.
- Ward, R.D., Burnside, N.G., Joyce, C.B., Sepp, K., 2016a. Importance of microtopography in determining plant community distribution in Baltic coastal wetlands. *J. Coastal Res.* 321, 1062–1070. <https://doi.org/10.2112/JCOASTRES-D-15-00065.1>.
- Ward, R.D., Teasdale, P.A., Burnside, N.G., Joyce, C.B., Sepp, K., 2014. Recent rates of sedimentation on irregularly flooded Boreal Baltic coastal wetlands: responses to recent changes in sea level. *Geomorphology* 217, 61–72. <https://doi.org/10.1016/j.geomorph.2014.03.045>.
- Ward, R.D., Burnside, N.G., Joyce, C.B., Sepp, K., Teasdale, P.A., 2016b. Improved modelling of the impacts of sea level rise on coastal wetland plant communities. *Hydrobiologia* 774 (1), 203–216. <https://doi.org/10.1007/s10750-015-2374-2>.
- Ward, R., Friess, D., Day, R., Mackenzie, R., 2016c. Impacts of climate change on global mangrove ecosystems: a regional comparison. *Ecosyst. Health Sustainability* 2 (4), 1–25. <https://doi.org/10.1002/ehs2.1211>.
- Westoby, M.J., Brasington, J., Glasser, N.F., Hambrey, M.J., Reynolds, J.M., 2012. 'Structure-from-Motion' photogrammetry: a low-cost, effective tool for geoscience applications. *Geomorphology* 179, 300–314. <https://doi.org/10.1016/j.geomorph.2012.08.021>.
- Yu, X., Hyyppä, J., Vastaranta, M., Holopainen, M., Viitala, R., 2011. Predicting individual tree attributes from airborne laser point clouds based on the random forests technique. *ISPRS J. Photogramm. Remote Sens.* 66 (1), 28–37. <https://doi.org/10.1016/j.isprsjprs.2010.08.003>.
- Zhang, W., Qi, J., Wan, P., Wang, H., Xie, D., Wang, X., Yan, G., 2016. An easy-to-use airborne LiDAR data filtering method based on cloth simulation. *Remote Sens.* 8 (6), 501. <https://doi.org/10.3390/rs8060501>.
- Zhang, H., Sun, Y., Chang, L., Qin, Y., Chen, J., Qin, Y., et al., 2018. Estimation of grassland canopy height and aboveground biomass at the quadrat scale using unmanned aerial vehicle. *Remote Sens.* 10 (6), 851. <https://doi.org/10.3390/rs10060851>.
- Zhou, H., Wang, X., Schaefer, G., 2011. Mean shift and its application in image segmentation. In: *Innovations in Intelligent Image Analysis*. Springer, Berlin, Heidelberg, pp. 291–312.
- Żmihorski, M., Krupiński, D., Kotowska, D., Knap, J., Pärt, T., Obloža, P., Berg, Å., 2018. Habitat characteristics associated with occupancy of declining waders in Polish wet grasslands. *Agric. Ecosyst. Environ.* 251, 236–243. <https://doi.org/10.1016/j.agee.2017.09.033>.
- Zuur, A., Ieno, E.N., Walker, N., Saveliev, A.A., Smith, G.M., 2009. *Mixed Effects Models and Extensions in Ecology with R*. Springer Science & Business Media.